Live cells assessment of opto-poration by a single femtosecond temporal airy laser pulse

G. Campargue,[1,a] B. Zielinski,[2] S. Courvoisier,[1] C. Sarpe,[2] T. Winkler,[2] L. Bonacina,[1] T. Baumert,[2] and J. P. Wolf[1]
[1]*Department of Applied Physics, University of Geneva, 1227 Carouge, Switzerland*
[2]*Institute of Physics and CINSaT, University of Kassel, 34132 Kassel, Germany*

(Received 24 July 2018; accepted 23 November 2018; published online 5 December 2018)

We report on the first study of live cell opto-poration by single temporally shaped femtosecond laser pulses. Based on an *ad hoc* developed cell staining protocol, we demonstrate the influence of the pulse temporal profile on the efficiency of poration and on cell viability at four hours comparing the results obtained for four different temporal pulse shapes: positive and negative temporal Airy, positively chirped, and 30 fs bandwidth limited pulses. Each pulse has been tested on a thousand cells. The most suitable pulses for opto-poration are the positive Temporal Airy Pulses (TAP+), likely because they enhance avalanche ionization compared to bandwidth-limited shorter pulses. We discuss the results in the context of previous studies, highlighting the differences between single and multi-pulse opto-poration strategies.
https://doi.org/10.1063/1.5049678

I. INTRODUCTION

Laser opto-poration is a method of choice for precise, gentle, and controlled delivery of molecules into cells as it avoids direct contact with the sample and does not require the use of chemicals or physical mediators. Laser pulses interact with cell membrane and the surrounding medium, which leads to the formation of a transient pore that allows uptake of exogenous molecules as large as DNA plasmids.

The first cell optoporation for gene delivery was reported by Tsukakoshi *et al.* in 1984 and was based on 5 ns laser pulses at 355 nm.[1] The technique was later improved thanks to the availability of mode-locked laser sources. Laser pulses were shortened considerably reaching the femtosecond range, and, in 2002, Tirlapur *et al.* reported successful femtosecond cell transfection.[2,3] Vogel *et al.* investigated both theoretically and experimentally the physical processes occurring around the intensity threshold required to produce a free electron density of approximately 10^{21} cm^{-3} in water (optical breakdown) and their influence on laser cellular nanosurgery.[4] Stevenson *et al.* focused expressly on viability and efficiency of transfection after optoporation. The transfection efficiency was found to be approximately 50% and cell viability of the transfected cells between 50% and 70%. These figures take into account the natural cell death and depend on the energy deposited per area.[5] The effect of irradiation parameters of high repetition-rate (MHz) sources were thoroughly screened in terms of pulse energy, intensity, and cumulative effects by several authors.[6–12]

This parameter screening was further extended by Davis *et al.*,[13] who evaluated the effect of 10^6 pulses with nJ energy against that exerted by two kHz higher energy pulses. Both approaches allowed successful poration and provided comparable results even though they rely on different interaction mechanisms. The former approach produces a low-density plasma. In this case, the poration is obtained by cumulative free-electron-mediated chemical effects. The second approach leads to

[a]Electronic mail: gabriel.campargue@unige.ch

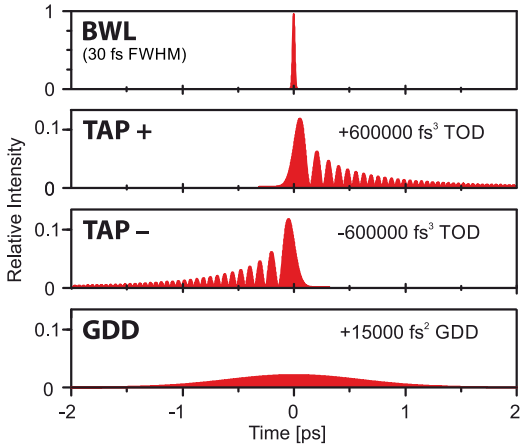

FIG. 1. Illustration of the four different pulses generated by our setup. TOD: Third Order phase Dispersion, GDD: Group Delay Dispersion. The energy is the same for each pulse. TAP+ and TAP– have the same peak intensity but TOD values of opposite sign. GDD parameter was chosen to achieve a temporal pulse length similar to TAP.

cavitation bubbles and subsequent membrane disruption in a few laser shots, as the interaction occurs at intensities above the optical breakdown in water.[4,13]

In the present study, we exploit this second interaction mechanism at high intensities, investigating for the first time the influence of the pulse temporal profile on poration efficiency and cell viability assessed after four hours within a single laser shot. We designed a protocol based on the interaction between cells and four kinds of ultrashort pulses with a wavelength centered around 785 nm and characterized by different spectral phase functions: 30 fs FWHM bandwidth-limited (BWL), positively chirped (GDD, for Group Delay Dispersion), and Temporal Airy Pulses with phases of both signs (TAP+ and TAP–). The temporal profile of each of these pulses is depicted in Fig. 1 (more details can be found in Ref. 14).

TAP+ has already demonstrated promising results in laser patterning of bulk materials such as fused silica,[14–16] where it was demonstrated that a single TAP+ can produce a hole with a much higher aspect ratio than a BWL pulse by exploiting the relevance of timing in the electronic excitation.[17] In 2016, we demonstrated their use for biological applications showing laser induced poration by TAP+ on fixed cancer cells.[18] TAP+ needs 22% of the BWL intensity in order to reach the same poration efficiency on fixed cells. Compared to BWL pulses, TAP+ leads to more controlled poration because it requires lower peak intensity to exert the same efficiency of poration. The physical origin of this difference resides in the multi-pulse structure of TAP+, where the leading sub-pulse (the most intense) starts the ionization and the subsequent sub-pulses trigger several avalanche ionization steps reaching the critical free electron densities for bubble formation much deeper in the material as compared to BWL pulses of the same energy by this "seed and heat" approach.[17,19,20]

In the following, after presenting the optical set-up and reviewing the staining protocol we designed, we compare the performances of the four pulse types in terms of poration efficiency and cell viability assessed after 4 hours and we discuss the results in the context of the literature addressing the effects of fluence and pulse shape.

II. METHODS

A. Optical set-up

Figure 2 presents the set-up that generated the different profiles displayed in Fig. 1. A one kHz amplified Ti:sapphire laser system (Femtolasers Femtopower Pro) provides 30-fs bandwidth limited (BWL) laser pulses at 785 nm. A Pockels Cell inside the amplifier allows to couple out a single pulse on demand. As shown in Fig. 2, the laser is guided through a home-built spectral phase modulator[21] used both for pre-compensating the dispersion introduced by transmissive optics (including the Zeiss N-Achroplan 40x, 0.75 NA, water immersion microscope objective) and imposing additional spectral

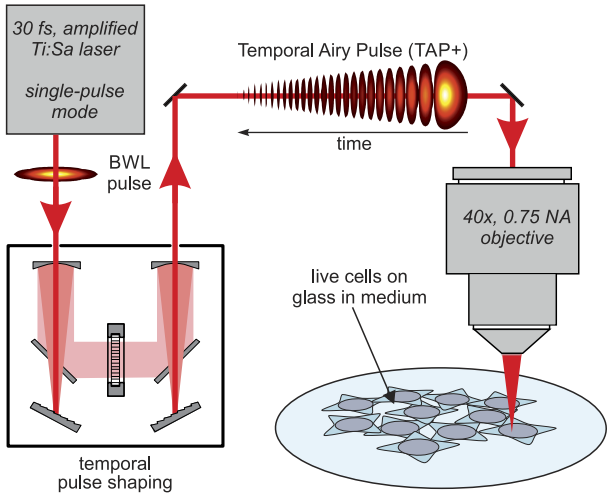

FIG. 2. Simplified scheme of the experimental set-up.

phase functions to the pulse. We assumed a 0.7 μm focal beam radius as the beam covers 50% of the objective pupil radius.[22] Temporal pulse characterization is performed via cross-correlation directly at the interaction site.[17]

Pulse energy is adjusted by a computer-controlled gradient neutral density filter wheel and measured by a photodiode. Before the measurement, the signal of the photodiode is calibrated against the reading of a cross calibrated powermeter (Ophir Nova II) placed directly at the objective's focal plane (without immersion medium).

B. Cell culturing

In terms of sample preparation, we cultured HeLa cells following standard methods recommended by ATCC. The cell culturing medium was composed of DMEM high glucose complemented with fetal bovine serum to a final concentration of 10% and 0.5 ml of 1x penicillin-streptomycin per 100 ml of final solution. The cells were incubated at 37°, 5% CO_2 in an open atmosphere system regulated by the incubator. The dispersed cells grow in an adherent monolayer on sterilized glass coverslips.

C. Poration protocol

The cell sample is placed on a (computer controlled) three-dimensional translation stage in a microscope setup (Fig. 2). An area with uniform cell layer is chosen by visual inspection under white light reflection microscopy.

During the experiment, arrays of 200 μm × 200 μm (≈160 cells) and 500 μm × 500 μm (≈1000 cells) were irradiated by a square grid of single pulses with 10 μm spacing in each direction. This corresponds to 1-3 possible spots for poration on each cell. As the adherent HeLa cells do not form a flat top layer, the focus of the collimated beam is positioned by a piezo translation stage at a fixed position of 6 μm above the confocally identified glass surface for all experiments. This distance was identified in our previous study with SEM as the most successful for poration of the top membrane.[18] Due to the natural differences in morphology among the cells, each shot focuses at a slightly different distance from the membrane. Thus, for each cell, it is likely to observe a combination of laser shots positioned differently. In order to allow direct comparison of efficiency and cell viability, we performed poration with all four pulse shapes on each sample.

D. Sample staining protocol

We used three fluorophores with distinguishable spectra in order to label all the relevant cell states at significative time points. After each administration of 2 ml of the dye solution, we incubated the cell sample for 30 minutes and finally, washed it with Dulbecco's Phosphate-Buffered Saline

(DPPS) for the green dye, or Dulbecco's Modified Eagle Medium (DMEM) for the blue and red dye. Figure 3A summarizes the timeline of the poration protocol and the table in Fig. 3B correlates cell states and final staining fluorophore signal. We applied:

- CellTracker CMF2HC (blue). This dye stains live cells and labels cells, viable before optoporation. The blue dye stock solution in Dimethyl sulfoxide (DMSO) was diluted in DMEM at a 1 μM concentration. In this work, we assumed that the dye keeps unchanged the threshold for electron plasma formation.
- LIVE/DEAD Fixable Green Dead Cell Stain Kit (L23101) (green). This fixable dye codes cells that have a damaged membrane: 1) dead cells, 2) cells with porated membrane. This fluorophore was expelled by the live cells after several hours of incubation. This green fluorescent probe stock solution (in DMSO) was diluted in DPBS without Ca^{2+} or Mg^{2+} at a 2 μM concentration. The sample was carefully rinsed with the same DPBS before adding live/dead fluo working

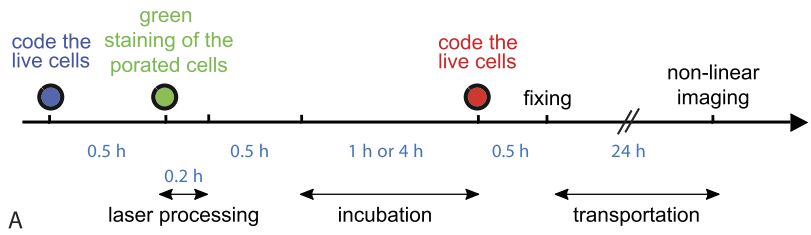

A

B

	Blue	Green	Red
Live cells before experiment	✓		
Live cells after incubation	✓		✓
Natural dead cells		✓	
Porated living cells	✓	✓	✓
Porated dead cells	✓	✓	

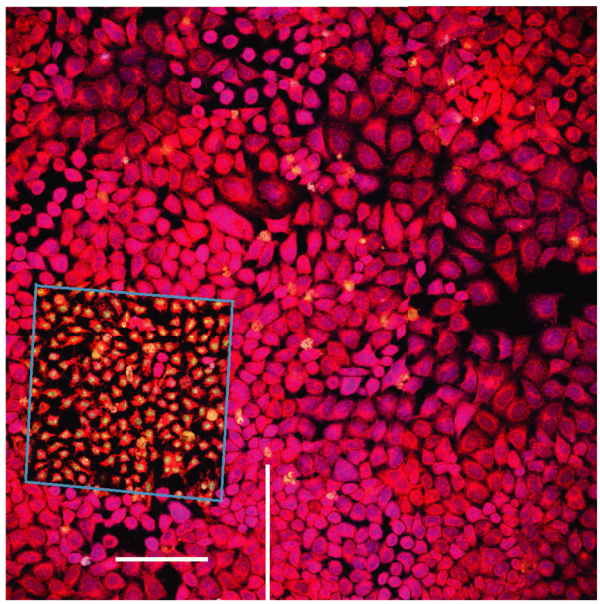

FIG. 3. (A) Timeline of the poration experimental protocol. (B) Table correlating cell states and final staining signal. (C) Example of an overlay of three fluorescent channels multiphoton microscopy images of a cell layer fixed after one hour of incubation, processed by BWL 100 nJ pulses. The blue square highlights the laser processed area. The white arrow indicates an example for a cell that was dead prior to poration (green coded only, which can be seen as yellow). Cells displaying red and blue fluorescence are alive but not porated. Successfully porated cells that are alive after one hour, display the signals associated with the three fluorescent probes (red, green and blue).

solution. For this fluorescent probe, the 30 minutes incubation time starts during the laser poration process.

- CellTracker CMTPX (red). This red probe stains the cells still living after membrane resealing following the poration experiment and incubation time. It allows differentiating between all the cells with a compromised membrane (dead or alive that were stained indifferently in green previously), as presented in Fig. 3B. The red dye stock solution in Dimethyl sulfoxide (DMSO) was diluted in DPBS at a 0.25 μM concentration.

In order to ensure that porations were successful immediately after the laser treatment, we added Calcein indicator for metal detection (CAS Number 1461-15-0) as a fluorescent marker for calcium to the medium right before laser poration and imaged the sample directly after by wide field fluorescence microscopy. This verification could not be done with L23101 marker, which is much slower at coding the damaged cells. Calcein (without acetoxymethyl) is not cell-permeable and its fluorescence is activated by presence of Ca^{2+}. The charged molecules of calcein cannot cross the untouched membrane of the cell. In the surrounding medium with almost no Ca^{2+} the calcein has a weak fluorescence. If the cell membrane is compromised, calcein enters the cell leading to bright fluorescence. However, the calcein is not retained in the cell cytoplasm and was not visible anymore after the one hour incubation time. After poration, incubation, and administration of the last fluorophore, we fixed the cells with a 4% solution of formaldehyde in DPBS.

E. Calculation of efficiency and viability

In order to characterize the effects of the laser treatment on cells, we define two conditions:

- A cell is considered **viable** if it is alive after being irradiated, irrespectively whether it is porated or not.
- A cell is considered **efficiently porated** if it is porated and alive after being irradiated and incubated during several hours.

TABLE I. Pulse duration, number of pulses ($N_{poration}$), peak intensity (I_{peak}), accumulated fluence (F_{acc}), transfection efficiency, delivery approach, and incubation time for the poration procedures reported in several recent articles using femtosecond laser pulses. The last rows present the characteristics of TAP+ and BWL pulses from this experiment, at 75 nJ. Two main different tendencies can be distinguished: MHz lasers with millions of pJ pulses and kHz lasers using a few pulses down to a single pulse in the nJ energy range. The efficiency is the *poration efficiency* as defined in current article, but different probes have been employed: GT: genetic transfection, MI: membrane integrity, NP: nanoparticles, NA: information not available. For the two items marked with the *, it corresponds to poration efficiency on fixed cells.[18] We advise some caution when directly comparing the entries in this dataset, as some authors do not mention whether the transfection efficiency has been corrected according to the culture proliferation or not. In addition the compared studies used different cell lines, molecules for transfection, and incubation time. Peak intensity for BWL pulses can be calculated with the formula $I_{peak} = \frac{E_{pulse}}{\Delta t\, A/2}$, where E_{pulse} is the energy per pulse, Δt the FWHM pulse duration, and A the focusing area ($1/e^2$ width). TAP values are taken from analytical solution (compare Fig. 1). The accumulated fluence is given by $F_{acc} = \frac{E_{pulse} \times N_{poration}}{A}$. Because we neglected (multi-photon) absorption by the biological medium, these calculations provide an upper limit of F_{acc} and I_{peak}.

Ref.	Pulse	$N_{poration}$	I_{peak} ($W \cdot cm^{-2}$)	F_{acc} ($J \cdot cm^{-2}$)	Efficiency	Probe	Incub. time
2,3	170 fs	$1.2\ 10^6$	$0.5 - 1.1\ 10^{12}$	$0.8 - 2.0\ 10^5$	100%	GT	72 h
6	10 fs	moving focus	$5.1\ 10^{13}$	$5.3\ 10^5$	NA	MI	NA
5	120 fs	$8 - 20\ 10^6$	$1.3 - 6.0\ 10^{12}$	$0.6 - 72\ 10^5$	40 – 60%	GT	48 h
24	100 fs	$0.8 - 4.0\ 10^5$	$1.7\ 10^{12}$	$0.5 - 3.4\ 10^4$	70%	GT	24 h
11	210 fs	$2.7 - 5.4\ 10^6$	$5.9 - 9.3\ 10^{12}$	$1.7 - 5.3\ 10^5$	0 – 70%	NP	90 min
12	20 fs	$3.8\ 10^6$	$0.6 - 7.9\ 10^{12}$	$0.5 - 5.9\ 10^5$	70 – 80%	GT	3 days
7	110 fs	$4.0\ 10^5$	$3.3 - 4.1\ 10^{11}$	$5.7 - 7.2\ 10^4$	79%	MI	12 h
25,26	200 fs	$3.2\ 10^6$	$0.4 - 5.4\ 10^{12}$	$2.1 - 2.5\ 10^5$	8 – 63%	GT	48 h
13	100 fs	$3.8\ 10^6$	$2.3 - 7.4\ 10^{12}$	$0.4 - 1.4\ 10^6$	30%	GT	24 – 48 h
13	100 fs	2	$0.5 - 1.5\ 10^{14}$	5.1 – 14.8	25%	GT	24 – 48 h
BWL18	30 fs	1	$3.2\ 10^{14}$	10	55% *	MI	fixed cells
TAP+18	1500 fs	1	$3.9\ 10^{13}$	10	70%*	MI	fixed cells
BWL	30 fs	1	$3.2\ 10^{14}$	10	33%	MI	4 h
TAP+	1500 fs	1	$3.9\ 10^{13}$	10	55%	MI	4 h

Hence, efficiently porated cells are a sub-ensemble of viable cells. Note that in this work we do not assess viability at longer times and possible cell apoptosis.

Low intensity and high fluence opto-poration studies showed that a percentage of the porated cells die during the incubation time.[5,11,12] In our work, all dead cells seem to be detached, and then washed out during the different steps of cleaning (before adding the red fluorophore and before fixation). Therefore, an efficiently porated cell is a porated cell that is not detached from the cell layer. However, a detached cell is not necessarily a dead cell meaning that the results as presented constitute a lower bound for viability assessment. A possible explanation for cell detachment is that, because under our working conditions laser fluence is very low and peak intensity much higher than in MHz repetition rate studies (see Table I), cavitation bubbles appear and apply a mechanical stress on the cell, which might induce a detachment without compromising cell viability.[4] Note also that the coverslips were not treated with special coating favouring cell adhesion.

By automated segmentation (Nikon Elements software), we count the number of porated cells and the density of cells in order to deduce the viability and efficiency of poration for each laser porated region of the sample. The number of detached cells is estimated comparing the cell density among laser treated and non-treated areas.

III. RESULTS

In Fig. 4, we present the relative proportion of porated live cells (in green), non-porated live cells (in red), and detached cells (in black) after laser treatment at two different pulse energies (75 nJ/pulse on the left and 250 nJ/pulse on the right). The laser treated area contained on average one thousand cells. The two-photon fluorescence imaging has been performed after four hours of incubation and fixation. As discussed below, these results demonstrate the clear influence of the laser pulse shape on poration and viability.

A. Efficiency of poration

The efficiency of poration at 75 nJ per pulse is higher for TAP+ than for the other temporal profiles we tested (55% for TAP+ versus 33% for BWL and no detection for TAP- and GDD). Pulse energy needs to exceed 200 nJ in order to porate with TAP- and GDD pulses (not shown here).

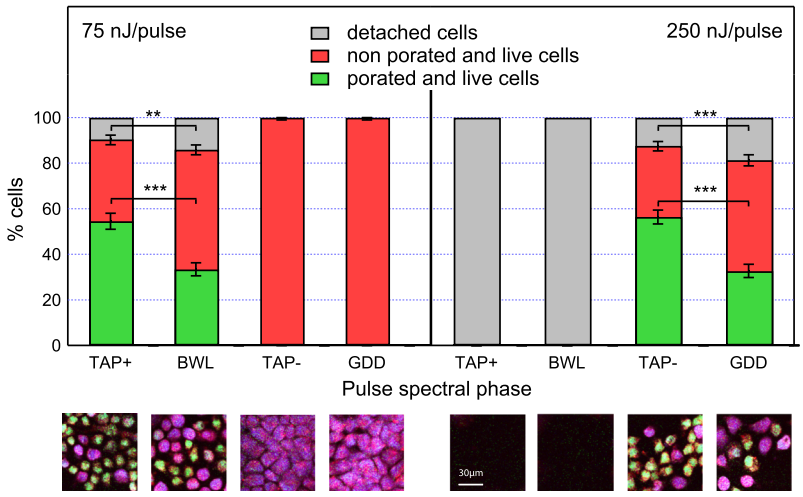

FIG. 4. *Top:* Poration efficiency and viability of HeLa cells after irradiation with single pulses at 75 nJ (*left*) and 250 nJ (*right*). For each laser processing condition, approximately 1,000 cells were treated. Measurements were performed after four hours of incubation. Porated and live cells (green) represent efficiently porated cells, whereas live cells (green and red) represents viable cells. Error bars have been calculated using a two-sided Agresti-Coull 95% confidence limits for a binomial proportion. *p*-values(***: $p < 0.001$, **: $p < 0.01$) were calculated by chi squared method. *Bottom:* Representative overlay of the three fluorescent channels measured by multiphoton microscopy images of laser scanned areas corresponding to the laser parameters presented on top. The scale bar is conserved between image.

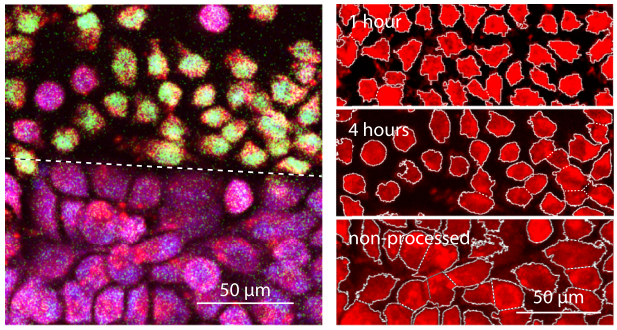

FIG. 5. *Left:* Overlay of three fluorescent channels multiphoton microscopy images of cell layers fixed after four hours of incubation, processed by BWL 75 nJ pulses (above the dashed white line) and non-processed (below the dashed white line). *Right:* Red fluorescent images of cell layers fixed after one hour of incubation (*top*), four hours of incubation (*middle*), and non-processed area (*bottom*). Scale bar is the same for the three images on the right. Non-processed and four hours incubation images correspond to left image. The porated cells seem to slowly recover their size over time as contraction is less notable after four hours of incubation (40% *versus* 50% of cell contraction after one and four hours respectively).

At 250 nJ they reach similar efficiencies as 75 nJ TAP+ and BWL pulses, but TAP- is more efficient than GDD pulses (56% versus 33%). At the same energy, BWL and TAP+ detach all the cells in the laser treatment area.

The data presented concurs with the results we previously obtained on fixed cells.[18] This preliminary study indicated similar poration efficiencies for TAP+ and BWL at low pulse energy and for TAP- and GDD at higher pulse energy. It was also observed that at high fluences, TAP- is at least as efficient in terms of single pulse poration as compared to TAP+ at low fluence.

B. Viability of the cells

Under our experimental conditions, the highest viability is obtained with TAP+ at 75 nJ/pulse (90%). At this energy, the viability of cells porated with BWL is just slightly lower at 86%. TAP− and GDD pulses at 75 nJ/pulse seem to not affect the cells: the viability is identical to that of the untreated area (100%). Conversely, for 250 nJ/pulse, the viability is 0% for TAP+ and BWL (no cells can be found in the treated area). At this energy, TAP− and GDD reach slightly lower viability (88% and 81%, respectively) than TAP+ and BWL at 75 nJ/pulse. For a given temporal profile, the viability is inversely correlated to the laser pulse energy (*i.e.* the more cells are detached from the layer).

We observe transient morphological changes of irradiated cells shortly after laser treatment (see Fig. 5). In fact, efficiently porated cells are strongly contracted to around 40% of the surface covered by the cell after one hour of incubation and return to 50% after four hours, which suggests that a slow size-recovery process is taking place.

IV. DISCUSSION OF THE RESULTS

The comparison of poration efficiency on live cells for all four pulse shapes confirm our earlier conclusions on fixed cells.[18] As we discuss in the following, TAP+ and BWL need significantly lower pulse energy to reach high poration efficiencies than TAP- or GDD. TAP+ seems to be the optimal choice for poration (highest efficiency and viability) at 75 nJ/pulse despite a much lower peak intensity than BWL.

A. Pulse duration dependence on efficiency of poration

At a given energy, TAP+ provides a better efficiency of poration than BWL for a similar cell viability, even if BWL reaches a peak intensity eight times higher. The peak intensity is usually presented as the driving parameter for poration efficiency. For TAP+, the leading, strongest sub-pulse starts the ionization and the trailing, weaker pulses are efficiently absorbed leading to avalanche ionization after several (at least eight[4]) inverse Bremsstrahlung events. Because of the time involved in this process, avalanche ionization is much less favourable in the case of BWL 30 fs pulses. In

fact, under these conditions, the dominant process is the generation of free electrons by strong-field ionization, meaning that the seed process is not followed by the electron heating.

Our previous works showed that TAP+ induce a laterally confined and longer axial range of high free electron density than BWL,[17,19,20] which suggests an easier poration for TAP+ despite cell-to-cell variations of the position of the outer membrane with respect to the laser focal point. Please note that under our conditions, at 75 nJ pulse energy, we work at two orders above the reported intensity threshold for bubble formation in water with fs pulses. Vogel *et. al.* reported that threshold to be in the 10^{12} W/cm^2 regime[4,23,30] whereas here we are in the 10^{14} W/cm^2 regime. TAP pulses show, in comparison to BWL pulses, only two to three times higher breakdown threshold.[19,20] As a consequence, all applied pulses should lead to the formation of a cavitation bubble, which is then defined by the distribution of electron density and thus by the applied temporal pulse shape. This suggests that bubble threshold arguments may be less important under our excitation conditions in comparison to the spatial extension under different pulse shapes.

B. Phase dependence

For a fixed energy, the two TAP pulses of positive and negative sign have the same peak intensity but TAP+ has a stronger effect on the cells. 250 nJ per pulse is needed for TAP- in order to reach the same efficiency of poration and viability than TAP+ at 75 nJ per pulse. The low peak intensity sub-pulses of TAP- are preceding (see Fig. 1) and are only weakly absorbed due to the nonlinear dependence of multi-photon ionization on intensity. The seed will hence be only available at later parts of the pulse and heating occurs only for a fraction of the trailing sub-pulses. Therefore, higher pulse energies for TAP- are needed to reach the same excitation and poration. A similar argument applies for GDD, a large part of the leading part of the pulse is just weakly absorbed and does not efficiently contribute to excitation.

C. Intensity and energy dependence on viability

The peak intensity plays a less important role in viability of cells than assumed with our study on fixed cells.[18] After four hours of incubation, despite an intensity eight times lower, TAP+ shows similar viabilities than BWL pulses. Hence, the weak correlation between intensity of the pulses and viability suggests that single pulse poration at high intensities is a good candidate for poration with high viability (see Table I).

In our previous work,[18] we observed a significant difference in the damage type on fixed cells. In particular, TAP+ was more likely associated with well-defined holes and TAP- with recess damage whereas both types were observed for BWL and GDD. The diameter of damage was in the range of 1 to 2 μm. Consistently with the present work, the energy necessary to induce a visible effect on cell membrane was found at least two-fold larger for TAP- than TAP+. We might ascribe the relative incidence of recess *vs.* defined ablation holes to the increased energy. Interestingly, here we do not observe difference in cell viability correlated with these two conditions.

One possible reason of the similar viability observed for TAP+ and BWL pulses, irrespectively of their significantly different efficiencies, is the size of the cavitational bubble. Indeed, the long temporal tail in TAP+ pulse might act enhancing the plasma density through the longer time span during which avalanche ionization occurs. Therefore, TAP+ may produce bubbles of size similar or larger than those generated by BWL pulses, which has an influence on the probability of membrane permeabilization. Such a scenario could be confirmed by carrying out scattering measurements for determining the size of the bubbles[23]).

D. Comparison with other femtosecond opto-poration methods

Most of the studies in the literature are based on opto-poration with millions of focused ultrashort pJ laser pulses at MHz repetition rate. Under these conditions, the peak intensity does not reach the threshold for the formation of cavitation bubbles and poration is governed by chemical bond disruption, release of free electrons, and heating.[4,13] In the present work, based on a single nJ pulse from a kHz regenerative amplifier, the poration is mainly governed by cavitation, and therefore directly correlated with free electron density, which, in turn, depends on pulse intensity and spectral phase.

Table I compares several poration conditions reported by various authors both from MHz and kHz regime, including.[24–26] We observe that the kHz approach is systematically associated with very low accumulated fluences (factor 10^4 – 10^8 smaller) leading to a substantial reduction of energy deposed on the sample (less linear absorption and heating). On the other hand, thanks to a higher intensity (10^2 larger), the poration efficiency is similar among all approaches (≈50%). Hence, one of the advantages of working with kHz laser systems at the limit of single pulse poration is the possibility to parallelize the interaction by spatially splitting a single mJ pulse with a microlens array or diffractive optics elements to increase the throughput of the poration procedure, in analogy to solutions recently proposed using plasmonic nanostructured substrates.[11,27–29]

V. CONCLUSION

With this work, we have demonstrated the influence of the spectral phase on live cell poration efficiency and viability using single femtosecond laser pulses. While TAP+ and TAP- provide similar poration efficiency and viability (exceding those associated with BWL and GDD pulses), TAP- needs significantly higher energies, which might lead to thermal energy deposition and induce some long term negative effects that are not observed after four hours of incubation. Overall, along the line of our previous studies on fixed cells,[18] at a fixed peak intensity, TAP+ is the most efficient pulse shape for opto-poration among the four we compared and especially better performing than the typically used BWL.

To our best knowledge, this work is also the first demonstration of a non-mediated (*i.e.* with no addition of chemicals or nanoparticles) poration of live cells with one single femtosecond pulse. The size of the hole previously measured on fixed cells suggests the possibility of exploiting the transient pores to deliver large molecules or plasmids. Because of the concurrent influence of other parameters in this process (*e.g.*, surface charge), *ad hoc* experiments are required to fully address this possibility.

The observation of a strong dependence between the temporal shape of the pulse and its interaction with the cell membrane and ambient media can lead to further investigations in the field of optical (nano)surgery and manipulation with such kind of pulses. For a detailed understanding of the underlying physical processes, the poration with high-intensity single (shaped) femtosecond laser pulses may be combined with time-resolved imaging experiments on single cells.

ACKNOWLEDGMENTS

We thank Markus Maniak (Department of Cell Biology of the University of Kassel) for support with cell culturing.

We received support from the German Research Foundation (DFG) within the priority program 1327 and from Otto Braun Fund for a PhD scholarship (Thomas Winkler).

[1] M. Tsukakoshi, S. Kurata, Y. Nomiya, Y. Ikawa, and T. Kasuya, "A novel method of DNA transfection by laser microbeam cell surgery," Applied Physics B **140**, 135–140 (1984).
[2] U. K. Tirlapur and K. König, "Targeted transfection by femtosecond laser," Nature **418**(6895), 290–291 (2002).
[3] U. K. Tirlapur and K. König, "Femtosecond near-infrared laser pulses as a versatile non-invasive tool for intra-tissue nanoprocessing in plants without compromising viability," Plant Journal **31**(3), 365–374 (2002).
[4] A. Vogel, J. Noack, G. Hüttman, and G. Paltauf, "Mechanisms of femtosecond laser nanosurgery of cells and tissues," Applied Physics B **81**(8), 1015–1047 (2005).
[5] D. Stevenson, B. Agate, X. Tsampoula, P. Fischer, C. T. A. Brown, W. Sibbett, A. Riches, F. Gunn-Moore, and K. Dholakia, "Femtosecond optical transfection of cells: Viability and efficiency," Optics Express **14**(16), 7125–33 (2006).
[6] V. Kohli, J. P. Acker, and A. Y. Elezzabi, "Reversible permeabilization using high-intensity femtosecond laser pulses: Applications to biopreservation," Biotechnology and Bioengineering **92**(7), 889–899 (2005).
[7] M. B. Zeigler and D. T. Chiu, "Laser selection significantly affects cell viability following single-cell nanosurgery," Photochemistry and Photobiology **85**(5), 1218–1226 (2009).
[8] M. Antkowiak, M. L. Torres-Mapa, F. Gunn-Moore, and K. Dholakia, "Application of dynamic diffractive optics for enhanced femtosecond laser based cell transfection," Journal of Biophotonics **3**(10-11), 696–705 (2010).
[9] C. McDougall, D. J. Stevenson, C. T. A. Brown, F. Gunn-Moore, and K. Dholakia, "Targeted optical injection of gold nanoparticles into single mammalian cells," Journal of Biophotonics **2**(12), 736–743 (2009).
[10] L. Gu and S. K. Mohanty, "Targeted microinjection into cells and retina using optoporation," Journal of Biomedical Optics **16**(12), 128003 (2011).
[11] J. Baumgart, W. Bintig, A. Ngezahayo, S. Willenbrock, H. M. Escobar, W. Ertmer, H. Lubatschowski, and A. Heisterkamp, "Quantified femtosecond laser based opto-perforation of living GFSHR-17 and MTH53 a cells," Optics Express **16**(5), 3021–31 (2008).

[12] A. Uchugonova, K. König, R. Bueckle, A. Isemann, and G. Tempea, "Targeted transfection of stem cells with sub-20 femtosecond laser pulses," Optics Express **16**(13), 9357–9364 (2008).
[13] A. A. Davis, M. J. Farrar, N. Nishimura, M. M. Jin, and C. B. Schaffer, "Optoporation and genetic manipulation of cells using femtosecond laser pulses," Biophysical Journal **105**(4), 862–871 (2013).
[14] M. Wollenhaupt, L. Englert, A. Horn, and T. Baumert, "Control of ionization processes in high band gap materials," Journal of Laser Micro/Nanoengineering **4**(3), 144–151 (2009).
[15] L. Englert, B. Rethfeld, L. Haag, M. Wollenhaupt, C. Sarpe-Tudoran, and T. Baumert, "Control of ionization processes in high band gap materials via tailored femtosecond pulses," Optics Express **15**(26), 17855 (2007).
[16] L. Englert, M. Wollenhaupt, C. Sarpe, D. Otto, and T. Baumert, "Morphology of nanoscale structures on fused silica surfaces from interaction with temporally tailored femtosecond pulses," Journal of Laser Applications **24**(4), 42002 (2012).
[17] N. Götte, T. Winkler, T. Meinl, T. Kusserow, B. Zielinski, C. Sarpe, A. Senftleben, H. Hillmer, and T. Baumert, "Temporal Airy pulses for controlled high aspect ratio nanomachining of dielectrics," Optica **3**(4), 389 (2016).
[18] S. Courvoisier, N. Götte, B. Zielinski, T. Winkler, C. Sarpe, A. Senftleben, L. Bonacina, J. P. Wolf, and T. Baumert, "Temporal airy pulses control cell poration," APL Photonics **1**(4), 046102 (2016).
[19] T. Winkler, C. Sarpe, N. Jelzow, L. Lasse H., N. Götte, B. Zielinski, P. Balling, A. Senftleben, and T. Baumert, "Probing spatial properties of electronic excitation in water after interaction with temporally shaped femtosecond laser pulses: Experiments and simulations," Applied Surface **374**, 235–242 (2016).
[20] C. Sarpe, J. Kohler, T. Winkler, M. Wollenhaupt, and T. Baumert, "Real-time observation of transient electron density in water irradiated with tailored femtosecond laser pulses," New Journal of Physics (2012).
[21] J. Köhler, M. Wollenhaupt, T. Bayer, C. Sarpe, and T. Baumert, "Zeptosecond precision pulse shaping," Optics Express **19**(12), 11638 (2011).
[22] H.-S. Chon, G. Park, S.-B. Lee, S. Yoon, J. Kim, J.-H. Lee, and K. An, "Dependence of transverse and longitudinal resolutions on incident Gaussian beam widths in the illumination part of optical scanning microscopy," Journal of the Optical Society of America A **24**(1), 60 (2007).
[23] A. Vogel, N. Linz, S. Freidank, and G. Paltauf, "Femtosecond-laser-induced nanocavitation in water: Implications for optical breakdown threshold and cell surgery," Physical Review Letters **100**(3), 1–4 (2008).
[24] L. Barrett, J. Sul, H. Takano, E. Van Bockstaele, P. Haydon, and J. Eberwine, "Region-directed phototransfection reveals the functional significance of a dendritically synthesized transcription factor," Nature Methods **3**(6), 455–460 (2006).
[25] P. Mthunzi, K. Dholakia, and F. Gunn-Moore, "Phototransfection of mammalian cells using femtosecond laser pulses: Optimization and applicability to stem cell differentiation," Journal of Biomedical Optics **15**(4), 041507 (2010).
[26] B. B. Praveen, D. J. Stevenson, M. Antkowiak, K. Dholakia, and F. J. Gunn-Moore, "Enhancement and optimization of plasmid expression in femtosecond optical transfection," Journal of Biophotonics **4**(4), 229–235 (2011).
[27] S. Courvoisier, N. Saklayen, M. Huber, J. Chen, E. D. Diebold, L. Bonacina, J. P. Wolf, and E. Mazur, "Plasmonic tipless pyramid arrays for cell poration," Nano Letters (2015).
[28] N. Saklayen, S. Kalies, M. Madrid, V. Nuzzo, M. Huber, W. Shen, J. Sinanan-Singh, D. Heinemann, A. Heisterkamp, and E. Mazur, "Analysis of poration-induced changes in cells from laser-activated plasmonic substrates," Biomedical Optics Express **8**(10), 4756 (2017).
[29] N. Saklayen, M. Huber, M. Madrid, V. Nuzzo, D. I. Vulis, W. Shen, J. Nelson, A. A. Mcclelland, A. Heisterkamp, and E. Mazur, "Intracellular delivery using nanosecond-laser excitation of large-area plasmonic substrates," ACS Nano **11**(4), 3671–3680 (2017).
[30] N. Linz, S. Freidank, X.-X. Liang, and A. Vogel, "Wavelength dependence of femtosecond laser-induced breakdown in water and implications for laser surgery," Physical Review B (2016).